

Neurocomputing Methods for Pattern Recognition in Nuclear Physics — Elastic Tracking *

M. Gyulassy¹ and M. Harlander²

Nuclear Science Division, Lawrence Berkeley Lab, Berkeley CA 94720

Abstract

We review recent progress on the development and applications of novel neurocomputing techniques for pattern recognition problems of relevance to RHIC experiments. The Elastic Tracking algorithm is shown to achieve sub-pad two track resolution without preprocessing.

1 Introduction

Experiments at RHIC will be confronted with difficult pattern recognition tasks due to the very high multiplicity of produced particles (see for example the RHIC proposals in Ref.[1]). In 1990, we initiated a generic R&D program to develop new computational strategies to help solve such problems based on numerical methods from the field of artificial neural networks[2]. One of the new results obtained was the development of a new tracking algorithm[3], Elastic Tracking (ET), that can extend tracking capabilities to much high densities than possible via conventional Road Finding or even previously proposed novel Hopfield network algorithms. This year we tested the tracking efficiency of ET on raw *unprocessed* ionization data[4]. In this paper we review the main results obtained in the above work.

2 Elastic Tracking

One of the physics objectives at RHIC is to measure the correlation function of identical particles in connection with pion interferometry[1]. This will require resolving tracks with very small momentum differences. To reduce effects due to Coulomb final state interactions it may be even necessary to resolve 3 or more overlapping mixed charge tracks with very small relative momenta. Present conservative estimates based on conventional Road Finding algorithms apparently limit the resolution to tracks separated by at least 3 pad widths. This limit arises because *local* tracking algorithms require a preprocessing stage in which the centroid of the local ionization density must be first determined. In Ref.[4] we demonstrated that significantly better resolution ($\sim \frac{1}{2}$ pad width track separation) is possible to achieve using the *global* strategy of the Elastic Tracking algorithm.

⁰*This work was supported by the Director, Office of Energy Research, Division of Nuclear Physics of the Office of High Energy and Nuclear Physics of the U.S. Department of Energy under Contract No. DE-AC03-76SF00098.

¹Speaker, Symposium on RHIC Detector R&D, BNL, Upton, L.I., NY, Oct. 9-10, 1991; Second Int. Workshop on Software Eng., A.I., and Expert Sys. for High En. and Nucl. Phys., L'Agelonde, France, Jan 13-18, 1992

²Permanent address: Technische Univ. München, Physics Department T30, James Franck Strasse 1, 8046 Garching, Germany.

ET is an adaptive template matching algorithm formulated in terms of dynamical systems. In [3] we considered tracking given preprocessed ionization source densities of the ideal form

$$\rho_S(x) = - \sum_a \delta(x - x_a) , \quad (1)$$

where x_a are track centroids. The problem of tracking is then to identify which subsets of points a should be linked together to form tracks. For multiple crossing tracks in the presence of noise, the combinatorial explosion of possibilities creates local ambiguities that can be only resolved by applying global algorithms such as ET. In [4] we extended the analysis to much more realistic densities of the form

$$\rho_S(\mathbf{x}) = \sum_{\alpha} \rho_{\alpha}(\mathbf{x}) , \quad (2)$$

where the density induced by track α is expressed as

$$\rho_{\alpha}(\mathbf{x}) = \int d\tau q(\mathbf{r}_{\alpha}(\tau)) \sigma(\mathbf{x} - \mathbf{r}_{\alpha}(\tau)) , \quad (3)$$

with $q(\mathbf{r}_{\alpha}(\tau))$ being proportional to the variable ionization charge density along the track. The finite range distribution, $\sigma(\mathbf{x})$, depends on the characteristics of the detector. On the average $\langle q \rangle$ is assumed to be proportional to the mean dE/dx of the particle. However, in physical detectors, Landau fluctuations cause large local fluctuations of q around that mean.

The α labels tracks according to the initial phase space point $\phi_{\alpha} = \{\mathbf{x}_{\alpha}, \mathbf{p}_{\alpha}\}$, on an allowed trajectory. We denote those trajectories by

$$\mathbf{r}_{\alpha}(\tau), \text{ where } \mathbf{r}_{\alpha}(0) = \mathbf{x}_{\alpha}, \quad d\mathbf{r}_{\alpha}(0)/d\tau = \mathbf{p}_{\alpha}/m , \quad (4)$$

for a particle of mass, m , produced at vertex position, \mathbf{x}_{α} , with momentum, \mathbf{p}_{α} . We assume that $\mathbf{r}_{\alpha}(\tau)$ is either known analytically, e.g., helices in a uniform magnetic field, or computable numerically from the known equations of motion, $m dp^{\mu}/d\tau = e F_{\alpha\beta}^{\mu\nu} p_{\nu}$, in the external EM field, $F_{\alpha\beta}^{\mu\nu}$, within the detector.

In [4] we also generalized the template charge distributions to allow for extended distributions of the form

$$\rho_T(\mathbf{x}) = q_T \int d\tau \sigma_T(\mathbf{x} - \mathbf{r}_T(\tau)) , \quad (5)$$

where q_T is the charge assigned to that template and where $\sigma_T(\mathbf{x})$ characterizes the shape of the template distribution around the trajectory $\mathbf{r}_T(\tau)$. For M templates, the total template charge density is simply the sum over the density of each.

Tracking in ET is performed by minimizing an effective energy for the combined source and template configuration

$$\rho(\mathbf{x}) = \sum_{\alpha=1}^N \rho_{\alpha}(\mathbf{x}) + \sum_{i=1}^M \rho_{T_i}(\mathbf{x}) . \quad (6)$$

The ET energy or cost function, $E(t)$, is simply a generalized “Coulomb” energy

$$E(t) = \frac{1}{2} \int d\mathbf{x} d\mathbf{x}' \rho(\mathbf{x}) V(\mathbf{x} - \mathbf{x}', t) \rho(\mathbf{x}') , \quad (7)$$

where $V(\mathbf{x}, t)$ is a finite range potential with a range that decreases slowly as a function of the *iteration* time. Any convenient finite range positive definite form can be used for the potential, e.g.,

$$V(\mathbf{x}, t) \propto \exp(-x^2/2w^2(t)) , \quad (8)$$

with

$$w(t) = (w_0 - w_f)e^{-\gamma t} + w_f . \quad (9)$$

The ET energy minimization task is performed via the gradient descent equations

$$d\mathbf{p}_i/dt = -\nabla_{\mathbf{p}_i} E(t) , d\mathbf{x}_i/dt = -\nabla_{\mathbf{x}_i} E(t) . \quad (10)$$

Starting from a random initial phase space point $\{(\mathbf{x}_i(0), \mathbf{p}_i(0)), i = 1, M\}$, the above equations evolve the phase space point specifying the template densities to one of the nearby minima of the interaction energy.

As in all optimization methods care must be taken to avoid getting caught in one of the many *local* minima of the energy surface. The strategy adopted in ET is the introduction of a slowly decreasing range, $w(t)$, of the effective potential as in eq.(9). The initial range, w_0 , should be taken to be large as compared with the average width of the measured distribution for an isolated track. The final width, w_f , should be less than that average width. The rate γ needs to be small compared to η so that (10) evolves adiabatically toward the global minimum. In the absence of fluctuations, i.e., $q(\mathbf{r}_\phi(\tau)) = \langle q \rangle$, the above algorithm always converges to the global minimum if $q_T = -\langle q \rangle$ and $\sigma_T = \sigma$.

The power of the ET algorithm is due to (1) that it utilizes all the known information about the class of allowed trajectories in a particular experimental device, (2) that no preprocessing of the measured ionization data is required, (3) that an *adaptive* non-linear χ^2 fit is automatically performed, (4) spurious minima are avoided by using a dynamical range, and (5) the output of ET is directly the quantity (x_T, p_T) of physical interest and thus no postprocessing is needed. See [5] for an alternate formulation of elastic tracking involving simulated annealing methods.

Figure 1 illustrates an application of ET to a 2D simulation of a TPC response for 2 and 3 overlapping tracks[4]. In this example, we assume a histogram form for the source $\sigma(x)$ to

simulate the image charge distributions on an array of pads in a TPC like detector [6]. All distances are measured in units of the pad width, Δx . Fig. 1. illustrates the source density in a $N = 20$ row detector for different track separations, d , as defined by the source separation on the row furthest from the common origin of the tracks. As our model of the response of a TPC we assumed that the source image charge distribution on pad i of row k is given by a clipped parabolic form:

$$\rho_{ik}^S = (-1 + \Delta q_{1k})[(i\Delta x - kd_1/N)^2 - w^2]_> + (-1 + \Delta q_{2k})[(i\Delta x - kd_2/N)^2 - w^2]_> , \quad (11)$$

where $[f]_> = f\theta(f)$ and $w = 1.2$. The d_i denote the crossing points of the track on row $N = 20$ and are simply related to the opening angle of the tracks ($\theta = |\tan^{-1}(d_1/N) - \tan^{-1}(d_2/N)|$). For the template density we thus take

$$\rho_{ik}^T = [(i\Delta x - kx_1/N)^2 - w^2]_> + [(i\Delta x - kx_2/N)^2 - w^2]_> . \quad (12)$$

As can be seen in Fig.1 ET is able to find the tracks even for 1/2 pad separations when local fluctuating ionization density is indeed ambiguous. The global view taken by ET is absolutely essential to resolve such local ambiguity. The average two track resolution, Δd , is shown in Fig. 2 for the case $\delta q = 0.75$ as a function of the their separation d at the outermost detector layer. The curves are labeled by the number of rows ΔN starting on row 20 toward the vertex which were taken into account in the analysis. The rapid rise of Δd for large d for the case $\Delta N = 1$ is due to an interesting phase transition as discussed in [4]. For sufficiently large number of readout layers though, Fig.2 shows that the global information is enough to achieve sub-pad resolution. Therefore we conclude that ET can extend tracking capabilities far beyond that which conventional local algorithms can achieve simply because all the measured and prior information is used at once. It thus enables one to approach the information theoretic limit of the detector.

3 Summary

New software approaches and computing algorithms will inevitably play a vital role in tracking and particle identification in high multiplicity RHIC, LHC and SSC detectors. We have shown an example of the power of such methods in connection with tracking small relative momentum tracks in a noisy TPC. Obviously many other applications can be envisioned[8]. Given unlimited resources, Mercedes or BMW type detectors can always be built with sufficient precision and efficiency that any old local information processing algorithm will suffice to process the data into useful physics. However, given finite resources, global neurocomputing optimization strategies make it possible to extract the last drop of useful information even from a VW scale experiment. In a nutshell, neurocomputing algorithms resolve locally ambiguous information by working on the global picture. Fast parallel hardware implementation of such algorithms

via VLSI [7] technology could turn even dumb apparati into smart detectors.

References

- [1] Fourth Workshop on Experiments and Detectors for a Relativistic Heavy Ion Collider, eds. M. Fatyga, B. Moskowitz, BNL 52262, UC-414, July 1990;
K. Kadija et al., An Experiment on Particle and Jet Production at Midrapidity, LBL-29651 (1990).
- [2] J. Hertz, A. Krogh, and R.G. Palmer, Introduction to the Theory of Neural Computation, Lecture Notes Vol. 1 Sante Fe Institute (Addison-Wesley Publishing Co, 1991).
- [3] M. Gyulassy and M. Harlander, Elastic Tracking and Neural Network Algorithms for Complex Pattern Recognition, Computer Physics Communications 66 (1991) 31.
- [4] M. Gyulassy and M. Harlander, High Resolution Multiparticle Tracking without Preprocessing via Elastic Tracking, LBL-31276 (1991), submitted to NIM B.
- [5] A. Yuille, K. Honda, and C. Peterson, Harvard Robotics Lab preprint 90-8 (1990); M. Ohlsson, C. Peterson, A.L. Yuille, preprint LU-TP-91-27 (1991).
- [6] G. Rai et al., IEEE Trans. on Nucl. Sci., 37 (1990) 56.
- [7] C. Mead, Analog VLSI and Neural Systems (Addison-Wesley Pub. Co., 1989).
- [8] I. Tserruya and H. Specht, et al, NA45 Collab, private communication; G. Paic et al (NA35 collab) Nucl. Phys. A525 (1991) 605c.

4 Figure Captions

- Fig. 1 Examples of the ionization density in a 2D simulation of a TPC like detector[6] with 20 layers and with local charge fluctuations $\delta q/q = 0.75$ at the pad level. The cases of two tracks with a separation $d = 0.5$ and 4.0 on layer 20 are shown. Top tick marks indicate location of crossing points of input tracks. The solid lines show the ET solution with a potential illustrated by the bell shaped curve on the center layer. Also an example of the response to 3 overlapping tracks is shown.
- Fig. 2 Relative two track resolution of ET[4] in pad units as a function of source separation for the 2-D example in Fig. 1 and for large local charge fluctuations with $\delta q/q = 0.75$. ΔN refers to the number of detector rows below and including row 20 that were included in the analysis.

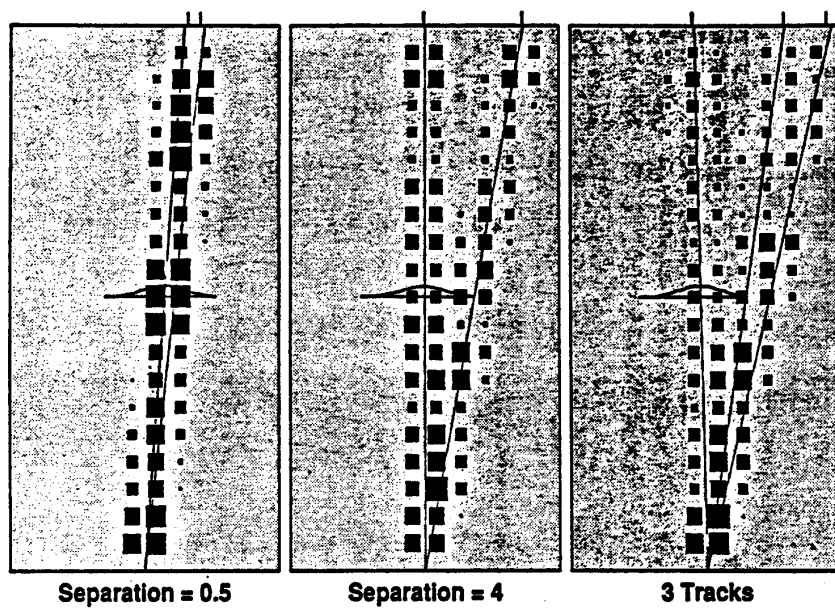


Fig. 1

2-D Tracking with $\delta q/q=0.75$

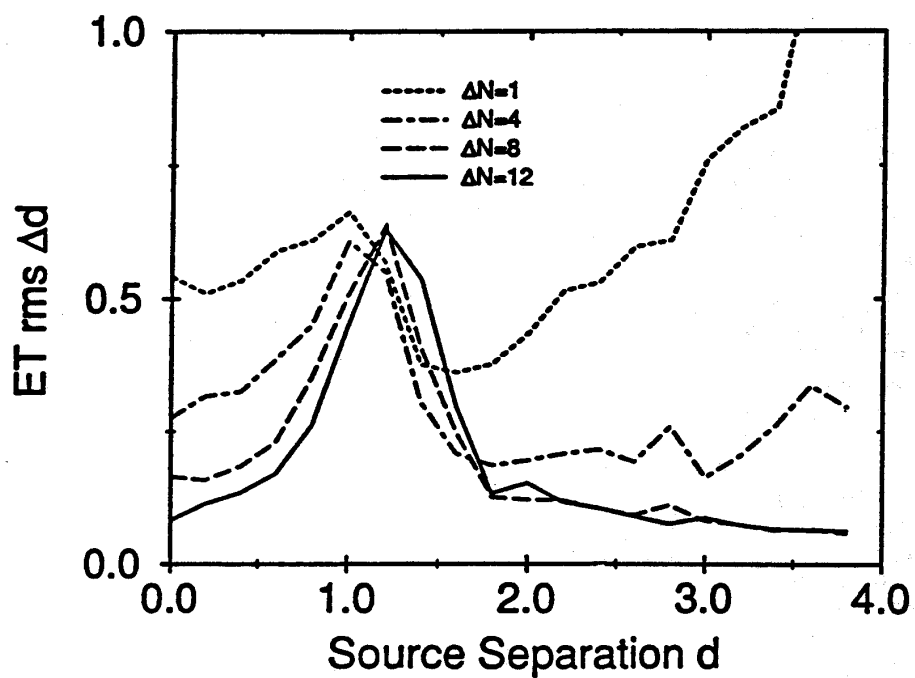


Fig. 2